
Article:
O'Brien, S., Kümmerli, R., Paterson, S. et al. (2 more authors) (2019) Transposable temperate phages promote the evolution of divergent social strategies in Pseudomonas aeruginosa populations. Proceedings of the Royal Society B: Biological Sciences, 286 (1912). ISSN 0962-8452

https://doi.org/10.1098/rspb.2019.1794

Transposable temperate phages promote the evolution of divergent social strategies in *Pseudomonas aeruginosa* populations

Siobhán O'Brien[1], Rolf Kümmerli[2], Steve Paterson[1], Craig Winstanley[3] & Michael A. Brockhurst[4]

[1]Institute of Integrative Biology, University of Liverpool, UK. L69 7ZB

[2] Department of Plant and Microbial Biology, University of Zürich, Switzerland

[3]Institute of Infection and Global Health, University of Liverpool, UK L69 7BE

[4]Department of Animal and Plant Sciences, University of Sheffield, UK. S10 2TN

Abstract

Transposable temperate phages randomly insert into bacterial genomes, providing increased supply and altered spectra of mutations available to selection, thus opening alternative evolutionary trajectories. Transposable phages accelerate bacterial adaptation to new environments, but their effect on adaptation to the social environment is unclear. Using experimental evolution of *Pseudomonas aeruginosa* in iron-limited and iron-rich environments, where the cost of producing cooperative iron-chelating siderophores is high and low, respectively, we show that transposable phages promote divergence into extreme siderophore production phenotypes. Iron-limited populations with transposable phages evolved siderophore over-producing clones alongside siderophore non-producing cheats. Low siderophore production was associated with parallel mutations in *pvd* genes, encoding pyoverdine biosynthesis, and *pqs* genes, encoding quinolone signaling, while high siderophore production was associated with parallel mutations in phenazine-associated gene clusters. Notably, some of these parallel mutations were caused by phage insertional inactivation. These data suggest that transposable phages, which are widespread in microbial communities, can mediate the evolutionary divergence of social strategies.

43 **Introduction**

44 Bacteriophages (phages) are viruses of bacteria, outnumbering eukaryotic viruses in
45 abundance and diversity (Reyes et al 2012). Phages have been found in almost all
46 environments studied so far, including human gastrointestinal (Breitbart et al 2003; Kim et al
47 2011) and respiratory tracts (Willner et al 2009). Phages can undergo lytic (killing the
48 infected host cell by lysis to transmit horizontally) or lysogenic cycles (integrating into the
49 host chromosome as a prophage to transmit vertically) (Little 2005; Ghosh et al 2009) and are
50 defined as either lytic or temperate depending on the absence or presence of a lysogenic
51 cycle, respectively. Whilst lytic phages have been shown to have wide-ranging ecological
52 and evolutionary effects on bacterial populations (Koskella and Brockhurst 2015), the
53 influence of temperate phages on bacterial evolution is less well understood.

54

55 Although temperate phages are capable of killing their bacterial host cell, integration into the
56 bacterial chromosome as a prophage can establish long-lasting relationships between phage
57 and bacterium (Harrison & Brockhurst 2017). Integration events may benefit the host by
58 fueling bacterial evolutionary innovation in two ways: First, accessory gene functions
59 encoded on the phage genome can provide or be co-opted to form new bacterial traits (e.g.
60 phage tail-derived bacteriocins (Strauch et al 2001)). Second, integration events *per se* can
61 increase the supply of mutations available to selection via insertional inactivation of bacterial
62 genes (Hulo et al 2015). For example, *mu*-like phages insert at random sites, generating
63 inversions, deletions, and integration between copies of itself, the chromosome and other
64 mobile elements (Toussaint & Rice 2017; Harrison & Brockhurst 2017). Infection of
65 *Pseudomonas aeruginosa* PAO1 with a *mu*-like phage (D3112) enhances the emergence of
66 antibiotic resistant colonies through insertional activation of *ami* genes (Rehmat & Shapiro
67 1983). The temperate phage LESϕ4 (closely related to *mu*-like D3112) was isolated from the

68 lung of a cystic fibrosis (CF) patient, and allows *Pseudomonas aeruginosa* to adapt faster to a
69 sputum-like environment, by increasing the supply of mutations available to *P. aeruginosa*
70 through prophage insertion into existing chromosomal genes (Davies et al 2016).
71
72 Studies showing that an elevated bacterial mutation rate can accelerate adaptation to the
73 social environment (Harrison et al 2005; 2007; O'Brien et al 2013), suggest that *mu*-like
74 phages could have a similar effect. Microbes produce a range of metabolically costly public
75 goods that increase their growth and survival, but which are open to exploitation by non-
76 producing 'cheats'. Siderophores, secreted by many bacterial species in response to iron-
77 starvation (Holden & Bachman 2015) are one example of a public good. Siderophore
78 production can be cooperative under nutrient-limited conditions, since it is individually costly
79 to make but the benefits are shared with neighboring cells (Griffin et al 2004; Butaite et al
80 2017; Sexton & Schuster 2017). Consequently, producing populations are vulnerable to
81 invasion by *de novo* non-producing cheats, who lose the ability to produce siderophores but
82 still retain the ability to use siderophores produced by others (Harrison & Buckling 2005,
83 2007; O'Brien et al 2013; Butaite et al 2017; Vasse et al 2015; 2017). Since cheating confers
84 a fitness advantage in this context, an increased supply of mutations available to selection can
85 increase the rate at which cheats evolve (Harrison & Buckling 2005, 2007). We hypothesize
86 that random integration events by the *mu*-like temperate phage LESϕ4, will similarly enhance
87 the supply of mutations, increasing the probability of cheats evolving.
88
89 Here, we examine the impact of a *mu*-like transposable temperate phage, LESϕ4, on the
90 evolutionary dynamics of siderophore cooperation in *P. aeruginosa*. Populations were
91 experimentally evolved in either iron-limited or iron-rich culture conditions where
92 cooperative siderophore production is, respectively, required or not required for growth. We

93 observed that, contrary to our prediction, transposable phage did not drive greater breakdown
94 of mean siderophore cooperation at the population level. In contrast, transposable phages did
95 promote greater divergence of siderophore production among bacterial clones, and thus led to
96 the coexistence of extreme social strategies within populations under iron-limitation.
97
98 **Materials and methods**
99 *a) Strains and culturing conditions*
100 We used *P. aeruginosa* PAO1 as our siderophore-producing wildtype ancestor, and the
101 temperate transposable phage LESϕ4. LESϕ4 inserts randomly into the host genome (Davies
102 et al 2016) and displays high rates of lytic activity in chronic CF lung infections, including
103 being induced into the lytic cycle by clinically relevant antibiotics (James et al 2015).
104
105 We confirmed that our PAO1 strain was susceptible to LESϕ4 using a plaque assay:
106 susceptibility was confirmed by a clear plaque on a bacterial lawn formed by phage-mediated
107 lysis. Evolution experiments were performed in casamino acids medium (CAA; 5g Casamino
108 acids, 1.18g $K_2HPO_43H_20$, 0.25g $MgSO_47H_20$ per litre). Media was made iron-limited
109 through the addition of sodium bicarbonate to a final concentration of 20mM, and 100ug ml^{-1}
110 of human apotransferrin. Iron-replete media was established by the addition of 20µM $FeSO_4$..
111 We confirmed that our iron rich conditions negated the fitness cost experienced by non-
112 producers under iron-limitation, by growing wildtype and a siderophore non-producing
113 mutant PAO1*ΔpvdDΔpchEF (*harbouring loss of function mutations in the two major
114 siderophores pyoverdine and pyochelin; Ghysels et al 2004) in iron-rich and limited media in
115 a 96 well plate, and measuring optical density (OD) after 24h (iron-rich: non-producers reach
116 higher densities than wildtype, t-test: t_{10}=3.7476, p=0.004; iron-limited: wildtype reach
117 higher densities than non-producers: Kolmogorov-Smirnov test: D=1, p=0.005). Wildtype

118 *per capita* pyoverdine production (see (c) below) was also repressed under iron-rich
119 compared with iron-limited conditions (Welch t-test: $t_{5.13}$=236.84, p<0.0001). The fitness
120 advantage experienced by non-producers in iron-rich environments has been attributed to the
121 cost of harbouring the siderophore producing machinery (Griffin et al 2004).
122
123 *b) Evolution experiment*
124 We followed real-time evolutionary changes in production of the most costly and efficient
125 siderophore, pyoverdine, over time (Visca et al 2007; Youard et al 2011; Dumas et al 2013),
126 in response to the present and absence of LESϕ4, in iron-rich and iron-limited CAA. To
127 ensure that each population was colonized by a single colony (i.e. relatedness =1 at the first
128 transfer), PAO1 was cultured in 6ml King's Medium B (KB; (10 g glycerol, 20 g protease
129 peptone no. 3, 1.5 g $K_2HPO_4 \bullet 3H_2O$, 1.5 g $MgSO_4 \bullet 7H_2O$, per litre) for 24h at 37°C, after
130 which it was diluted with M9 minimal salt solution and grown for 24h on KB agar at 37°C. A
131 single colony was then selected and grown in KB medium at 37°C for 24h, and subsequently
132 used to establish populations.
133
134 To initiate the experiment, twelve 30ml universal glass tubes were filled with 6ml iron-
135 limited CAA, and twelve with iron-rich CAA. PAO1 was inoculated to a density of 5 x 10^6
136 CFU ml^{-1}. 10^6 ml^{-1} plaque forming units (PFU's) of LESϕ4 phage was added to six iron-
137 limited and six iron-rich populations (MOI=1), in a full factorial design. Cultures were grown
138 shaken at 180rpm with slightly loose caps, at 37°C.
139
140 Every 24h, 1% of each population was transferred to fresh tubes (iron-rich or limited as
141 appropriate). The experiment was conducted for 30 transfers, and every 2nd transfer
142 populations were mixed with 20% glycerol and frozen at -80°C for further analysis. At

143 transfers 10, 15, 20, 25 and 30, populations were 1) plated on KB agar to assess density
144 (colony forming units (CFU) /ml), and 2) tested for the presence of free phage.
145
146 *c) Pyoverdine Assays*
147 Every 10 transfers, populations were diluted and plated on KB agar. Thirty colonies from
148 each population were selected at random, and pyoverdine production quantified for each
149 colony (2160 colonies total). Using sterile toothpicks, individual colonies were transferred to
150 120µl KB medium in 96 well plates. Plates were incubated static for 24h at 37°C to
151 approximately equalize densities across cultures. 1% of each culture was then transferred to
152 180ul iron-limited CAA (siderophore-stimulating conditions), and incubated static for 24h at
153 37°C. Colonies were analysed for pyoverdine production (RFU) using a pyoverdine-specific
154 emission assay (Ankenbauer et al 1985; Cox & Adams 1985). Briefly, fluorescence emission
155 of each culture was measured at 460nm following excitation at 400nm, using a Tecan infinite
156 M200 pro spectrophotometer. Optical density (OD) was also measured at 600nm, and the
157 ratio RFU/OD was employed as a quantitative measure of per capita pyoverdine production
158 (Kümmerli et al 2009 JEB). Nonproducers were classified as those colonies producing <5%
159 ancestral pyoverdine levels (<6069.25 RFU). Overproducing colonies were in the 95th
160 percentile (> 146,590 RFU) for per capita pyoverdine production. Ancestral per capita
161 pyoverdine was 121,385 RFU.
162
163 *d) Sequencing evolved clones*
164 To identify the underlying genetic drivers of siderophore cheating in the iron-limited phage
165 treatment, we specifically selected the two highest pyoverdine producers and two lowest
166 producers from each population evolving in this treatment. Since the proportion of
167 siderophore producers relative to non-producers did not always permit this at the final

168 transfer, clones were isolated from the iron-limited phage treatment at either the 10th
169 (Populations 2,5 and 6) or 30th (Populations 1,3 and 4) transfer. To test whether observed
170 parallel mutations in these clones are treatment-specific, we next selected 4 clones at random
171 from every population in the remaining treatments at the final timepoint (72 clones from 18
172 populations).
173
174 The Wizard® Genomic DNA Purification kit (Promega) was used to isolated genomic DNA
175 from overnight cultures, according to the manufacturer's instructions. The quality and
176 quantity of the isolated gDNA was assessed using Nanodrop (Thermo Scientific) and Qubit,
177 respectively. Illumina Nextera XT genomic libraries were prepared by the Centre for
178 Genomic Research, University of Liverpool and 2 × 250 bp paired-end reads generated on an
179 Illumina MiSeq platform.
180
181 Reads were aligned to the PA01 reference (NC_002516.2) using BWA-MEM (Li, 2013),
182 duplicates removed and variants detected and filtered using the Genome Analysis Toolkit
183 (GATK) HaplotypeCaller and VariantFiltration tools (McKenna et al 2010) based on GATK
184 filtering recommendations. Mutations common to all clones were removed from dataset, as
185 these likely represented divergence between our PAO1 stock and the reference genome.
186 Only variants passing filtering were included in the final dataset (196 mutations across all
187 clones). A further 75 were mutations associated with pf1 bacteriophage. Mutations in Pf1
188 were present in all 96 sequenced genomes and are therefore likely to be a response to the
189 laboratory environment, rather than selection imposed by phage or iron in our experiment.
190 Hence these mutations were removed from further analysis. Of the remaining 121
191 mutations, 12 were synonymous and were excluded from analysis. The remaining 109
192 mutations comprised our final dataset, consisting of frameshifts (33%), missense mutations

193 (49%), gene deletions (13%) and stop-gained (6%). Evolved clones acquired between 15
194 and 32 non-synonymous mutations each, with a mean of 16.47 mutations per clone. We
195 further analysed the data to pinpoint the genes in which phage had inserted (SNP calling
196 does not detect phage-mediated mutations; Davies et al 2016). All reads were mapped to
197 the PA01 and phi4 genomes and reads retained where one member of a read pair mapped to
198 PA01 and the other to phi4. From these, reads mapping to the PA01 genome were counted
199 within 1kbp moving windows and potential insertion sites further inspected in IGV
200 manually (Thorvaldsdóttir et al 2013). Phage insertion sites were identified in all 48 phage-
201 evolved clones isolated from 12 populations.
202
203 *e) Statistical analysis*
204 All data were analysed using R version 2.15.1 (R Core Team, 2016). We used a t-test (for
205 normally distributed data and equal variances) and Kolmogorov Smirnov test (non-normal
206 distribution and unequal variances) to compare Malthusian growth rates (*m)* of each strain
207 under iron rich and iron limited conditions, respectively. Malthusian growth rate (*m)* was
208 quantified as ln(Final density/Starting density) (Lenski et al 1991). We used linear mixed
209 effects models to investigate how iron limitation and phage presence influenced a) per capita
210 pyoverdine production, b) variance in pyoverdine production c) population density and d)
211 numbers of overproducers, over the course of the experiment (table S4). The effect of phages
212 and iron on population density after 24h growth was tested using a 2-way anova. Finally,
213 after ensuring high and low producers did not differ in the variance of nonsynonymous
214 mutations (permutational ANOVA, permutation test: $F_{1,10} = 0.5373$, $P = 0.491$), we
215 performed a Permutational Multivariate Analysis of Variance using the adonis function in R
216 to assess mutational differences between phenotypes (Anderson 2001).
217

218 **Results**

219 *a) No effect of temperate phages on population densities*

220 While free phage particles were detected in all populations from phage treatments throughout
221 the experiment, the presence of phages had no effect on bacterial densities, either over the
222 course of the experiment (LMER; $X^2_{1,6}$= 0.1698, p=0.68, figure S4), or after 24h growth with
223 or without phages (F=3e-04, p<0.98). This suggests that any observed differences between
224 treatments propagated with or without phages were unlikely to have been primarily driven by
225 the ecological effects of phage-killing (Vasse et al 2015).

226

227 *b) The evolutionary dynamics of pyoverdine production*

228 To obtain a quantitative measure of siderophore production, we calculated *per capita*
229 pyoverdine production for thirty colonies per population every 10th transfer for 30 transfers.
230 Iron limitation reduced *per capita* pyoverdine production, but this effect weakened over time
231 (LMER; iron x transfer interaction, $X^2_{1,9}$= 8.1656, p=0.004, figure 1, figure S3). To a lesser
232 extent, transposable phage presence also reduced *per capita* pyoverdine production, but
233 again, this effect became weaker over time (LMER; phage x transfer interaction, $X^2_{1,9}$=
234 4.2632, p=0.03, figure 1, figure S3). The degree to which iron limitation affected pyoverdine
235 production was not influenced by the presence of phage over the course of the experiment, or
236 *vice versa* (LMER; non-significant iron x phage x transfer interaction, $X^2_{1,11}$= 0.0003, p=0.9,
237 figure 1, figure S3).

238

239 Within-population variance in pyoverdine production was highest in iron-limited populations
240 evolving with phages (LMER; phage x iron interaction, $X^2_{1,9}$=12.22, p=0.0004, figure 2,
241 figures S1-S3), irrespective of time (LMER non-significant phage x iron x transfer interaction
242 $X^2_{1,11}$=0.4591, p=0.4981, figure 2, figures S1-S3). Neither iron-limitation nor phage presence

243 alone influenced within-population variance (LMER; iron effect $X^2_{1,6}$= 1.19, p=0.27; phage
244 effect $X^2_{1,6}$= 2.99, p=0.08, figure 2, figures S1- S3), indicating that variation is maximized by
245 social exploitation in the presence of phage.
246
247 To determine whether this higher variance was driven by increased numbers of pyoverdine
248 over-producers, non-producers, or coexistence of both, we analysed the number of non- and
249 overproducing clones in each treatment. Numbers of overproducing clones increased in the
250 presence of phage over time (phage x timepoint interaction: $X^2_{1,7}$= 5.2866, p=0.022), and this
251 was not significantly influenced by iron availability (effect of iron: $X^2_{1,7}$= 5.2866, p=0.4).
252 Equivalent results were obtained using different cut-off values for over-production (phage x
253 timepoint interaction, 75th: $X^2_{1,8}$ = 5.54, p=0.01, 80th: $X^2_{1,7}$ = 5.78, p<0.05, 85th: $X^2_{1,8}$ = 4.3736,
254 p<0.05, 90th: $X^2_{1,8}$ = 4.5, p<0.05) suggesting that our observation that the frequency of
255 overproducers increased over time in the presence of phage is robust.
256
257 Nonproducing clones (n=17) were identified throughout the experiment, predominantly (in
258 15/17 cases) in iron-limited populations evolving with phages (Table S1). By the final
259 transfer, nonproducing mutants had been observed at least once in 5/6 populations from the
260 iron-limited treatment with phages. Together, this suggests that the increased variation in
261 pyoverdine production observed in the iron limited populations evolved with phages was
262 driven by increased numbers of pyoverdine nonproducers in this treatment in addition to
263 increased numbers of overproducers driven by the presence of phage *per se.*
264
265 *c) Genome sequencing of evolved clones*
266 To examine the genetic bases of the observed divergence in pyoverdine production
267 phenotypes observed in iron-limited populations evolved with phages, we obtained whole

268 genome sequences for the two highest- and the two lowest-pyoverdine-producing clones
269 from each population (i.e. 24 clones; 4 clones each from 6 populations). Comparing the
270 highest- (n=12) and lowest-producing clones (n=12), we sought to identify mutations
271 distinguishing these classes. First, we analysed all nonsynonymous mutations, including
272 SNPs and indels together with genes affected by phage insertional inactivation mutations.
273 High and low producers did not differ in the variance of nonsynonymous mutations
274 (permutational ANOVA, permutation test: $F_{1,10} = 0.5373$, $P = 0.491$), but the loci affected
275 by non-synonymous mutations did differ between high and low producers (permutational
276 ANOVA, permutation test: $F_{1,10} = 2.1429$, $P = 0.014$, Figure 3, Table S2).
277
278 To identify loci likely to have been under divergent positive selection between high and low
279 producers, we looked for evidence of phenotype-specific parallel evolution, i.e. pathways
280 targeted by mutation in multiple clones isolated from independently evolving replicate
281 populations that occurred exclusively in either high or low pyoverdine producers. In low
282 producing clones, we observed parallel mutations in quorum-sensing associated loci (*pqsA,*
283 *pqsR*; 3/6 populations; 5 clones, Figure 3A,B, Figure 4, Table S2) and pyoverdine
284 biosynthesis associated loci (*pvdA, pvdD, pvdI, pvdS* binding site; 4/6 populations; 8
285 clones, Figure 3A,B, Figure 4, Table S2). Notably, two of these parallel mutations were
286 caused by prophage-mediated insertional inactivation into *pqsA* and *pvdD* genes,
287 respectively. Furthermore, while clones with *pqs* mutations produced less pyoverdine than
288 the ancestor (figure 4), clones harbouring both *pvd* and *pqs* mutations did not produce any
289 detectable pyoverdine (figure 4).
290
291 Exclusive to the highest-producing clones, we observed parallel mutation of a phenazine
292 (*phz*)-associated intergenic region in 2/6 populations (3 clones), all of which were caused

293 by prophage insertion (Figure 3A,B, Figure 4, Table S2). These patterns of distinct parallel
294 evolution in high and low producers are suggestive of divergent selection in the iron-
295 limited populations evolving with phages, and, furthermore, shows that prophage-mediated
296 insertional inactivation mutations contributed to the response to this divergent selection. In
297 addition, we observed shared targets of parallel evolution in flagella associated genes (*flgE,*
298 *flgF, flgG, flgJ, fliF, fliI*) in both highest- (2/6 populations; 3 clones) and lowest-producer
299 clones (4/6 populations; 7 clones). This suggests that impairment of flagellar motility was
300 beneficial *per se* in our experimental setup, and, moreover, since all but one of these
301 mutations were caused by prophage insertional inactivation, that transposable phage mediated
302 this response to selection.
303
304 Next, to determine whether the identified targets of parallel evolution were specific to the
305 iron-limited populations evolved with phages, we obtained whole genome sequences for 4
306 randomly chosen evolved colonies from each of the replicate populations from the other
307 treatments (Table S3). Because, in these treatments, variation among clones in siderophore
308 production was less extreme, colonies from these populations were chosen at random (instead
309 of selecting high and low producers). Importantly, we never observed mutations in *pqs, pvd*
310 or *phz* associated loci in any of these other treatments. This suggests that mutations in *pqs*,
311 *pvd* or *phz* associated loci predominantly occurred in iron-limited populations evolved with
312 phages, indicating that these populations followed an evolutionary direction distinct from
313 both iron-rich populations and iron-limited populations evolved without phages.
314
315 Populations evolved in iron-rich environments underwent highly parallel evolution of the
316 quorum sensing master regulator *lasR*, with 12/12 populations acquiring nonsynonymous
317 SNPs or indels irrespective of phage presence or absence. *lasR* mutations were never caused

318 by prophage insertional inactivation and were never observed in the iron-limited
319 environment, suggesting that loss of *lasR* was an adaptation to iron-rich conditions and was
320 unaffected by the presence or absence of phages. Mutation of flagella-associated loci was
321 observed in all iron-rich populations irrespective of whether phages were present or absent,
322 confirming that loss of flagellar motility is likely to be adaptive *per se* in this well-mixed
323 laboratory environment. When phage was present, prophage-mediated insertional
324 inactivation was the primary mode of flagella-associated mutation, occurring in all 6 replicate
325 populations. Interestingly, under iron limitation, the increased mutational supply provided by
326 transposable phage insertion appears to have promoted loss of flagellar motility: Mutation of
327 flagella-associated loci was not observed in iron-limited populations evolved without phage,
328 in contrast to iron-limited populations evolved with phage where such mutations were
329 common and frequently associated with prophage insertional inactivation (described above).
330

331 **Discussion**

332 Transposable phages increase the supply of mutations and thereby can accelerate bacterial
333 adaptation to a new environment (Davies et al 2016). Here, we show that as well as
334 enhancing the response to abiotic environmental selection, transposable phages can also
335 mediate evolutionary responses to the social environment. Populations evolving with phages
336 in an iron-limited environment requiring cooperative siderophore production followed a
337 distinct evolutionary trajectory compared both to populations in the same environment
338 evolved without phages and to populations evolved with or without phage in an iron-rich
339 environment not requiring cooperation. Specifically, within iron-limited populations evolved
340 with phage we observed greater variation in pyoverdine production among bacterial clones.
341 This was caused by a combination of more overproducing mutants evolved in populations
342 with phage (irrespective of iron availability), and the evolution of more under-producing and

343 non-producing mutants in the iron-limited populations with phage, specifically. Our results
344 suggest therefore that transposable phage promoted the evolutionary divergence of the
345 population into more extreme social strategies.
346
347 We examined the genetic basis of divergence between the highest- and lowest-producing
348 clones that evolved in the iron-limited treatment with phage. In the lowest-producer class,
349 we observed that pyoverdine synthesis (*pvd*) and regulators of PQS quorum sensing *(pqs)*
350 associated loci were repeatably targeted by parallel mutations in independent replicate
351 lines. Mutation of *pvd*- loci encoding pyoverdine synthesis can cause reduced pyoverdine
352 production (Lamont & Martin 2003; Kümmerli et al 2015; Granato et al 2018, this study
353 (figure 4)) and are likely to explain low pyoverdine production in some clones. However, *pvd*
354 mutations were not universal among low pyoverdine producers, and one of the evolved
355 clones from the highest-producer class also carried a *pvd* mutation and maintained ancestral
356 levels of pyoverdine production (Table S2). It is likely therefore, that *pqs* mutations also
357 played a role in the evolution of reduced pyoverdine production. Consistent with this, *P.*
358 *aeruginosa pqsR* null-mutants produce reduced pyoverdine compared with wildtype (Popat et
359 al 2017; this study (figure 4)), and we could not detect any pyoverdine production in clones
360 harbouring both *pqs* and *pvd* mutations (figure 4). Interestingly, the PQS signal molecule acts
361 as an iron-chelator, so loss of PQS quorum sensing would increase the relative availability of
362 iron, reducing the need for siderophore production (Diggle et al 2007; Popat et al 2017).
363
364 Exclusive to the highest-producing clones, we observed parallel mutation of a phenazine
365 (*phz*)-associated intergenic region, mediated by prophage insertion between *phzG2-*
366 *PA1906*, and *phzG1-phzS*. *P. aeruginosa* operons phzA1-G1 and phzA2-G2 are involved in
367 biosynthesis of the pyocyanin precursor, phenazine-1-carboxylic acid (PCA). The intergenic

368 region *phzG2-PA1906* contains a putative transcriptional terminator 30bp downstream of
369 the *phzG2* stop codon, and the intergenic region directly downstream of the *phz1* cluster
370 (*phzG1-phzS*) contains a ribosome binding site (Mavrodi et al 2001). Hence, it is likely that
371 these mutations impede both stability and efficiency of the translated phenazine product.
372 Since pyocyanin increases iron-availability by reducing Fe^{3+} to bioavailable Fe^{2+} (Cox
373 1986) it is possible that high pyoverdine production in these mutants is a response to
374 reduced iron availability caused by reduced levels of the pyocyanin precursor PCA
375 (Granato et al 2018). Interestingly, *pqs* mutations in low pyoverdine producers were always
376 found in the same populations as clones with *phz* mutations – hence, it is possible that *pqs*
377 mutations in under-producing clones are a response to, or a driver of, *phz* mutations in
378 coexisting over-producing clones.
379
380 Adaptation to the iron-rich environment was associated with acquisition of nonsynonymous
381 SNPs or indels in *LasR*, the master regulator of acyl-homoserine lactone (AHL) quorum
382 sensing. This pattern was irrespective of phage, occurring both in their presence or absence,
383 and the mutations were not mediated by prophage insertion. Loss of AHL quorum sensing
384 is a common adaptation to the CF lung (Smith et al 2006; Fothergill et al 2007; LaFayette et
385 al 2015; Davies et al 2016), the *Caenorhabditis elegans* gut (Granato et al 2018; Jansen et al
386 2015) as well as laboratory media (O'Brien et al 2017; Granato et al 2018). Similarly, loss of
387 *lasR* in CAA is unsurprising – *lasR* is costly and not required in CAA (Sandoz et al 2007;
388 Diggle et al 2007; Darch et al 2012; Ghoul et al 2014). Ghoul et al (2014) demonstrated that a
389 *lasR* mutant grows faster than the wildtype producer in CAA, both when grown alone and in
390 direct competition – showing that mutations in this region are beneficial *per se*. However,
391 while we found *lasR* mutations in 12/12 populations evolving under iron-rich conditions, this
392 was never observed under iron-limitation. This may be because *lasR* expression is enhanced

393 by iron-limitation (Bollinger et al 2001), suggesting that functions regulated by LasR are
394 beneficial in this environment. An alternative explanation is that iron limited populations
395 failed to undergo *lasR* mutations because their densities were lower and their evolutionary
396 potential was correspondingly decreased compared with iron rich (Figure S4). However, even
397 under iron limited conditions, populations reached 10^8-10^9 CFU's/ml, which is roughly
398 tenfold higher than that observed in CF artificial sputum – conditions under which *lasR*
399 mutations are commonly observed (Davies et al 2016). Hence, density alone is unlikely to
400 explain the lack of *lasR* mutation under iron-limited conditions.
401
402 Previous studies suggest that the ecological effects of phage-killing can influence siderophore
403 production (e.g. O'Brien et al 2013; Vasse et al 2015). Vasse *et al* (2015) reported that
404 LKD16 lytic phages of *P. aeruginosa* select for pyoverdine non-producers, both in the
405 presence and absence of iron. Similarly, O'Brien *et al* (2013) found that *Pseudomonas*
406 *fluorescens* SBW25 non-producers grow better than producers in the presence of the lytic
407 bacteriophage φ2 under iron limited conditions. This latter finding was explained by the 'kill
408 the winner' hypothesis – the rate of killing is enhanced for the most prevalent genotype, so
409 there is a fitness advantage to being rare. Although LESφ4 is capable of both lytic and
410 lysogenic infection (James et al 2012; 2015), and we found evidence of lysis throughout our
411 experiment, similarly to Davies et al (2016) we observed no effect of LESφ4 on bacterial
412 densities either in the short-term or during the long-term experiment. This suggests that the
413 ecological effect of phage-killing are unlikely to explain our finding that transposable phage
414 promote the evolution of both higher and lower siderophore production under iron-limitation.
415
416 Flagella-associated mutations were common in our shaken liquid cultures, frequently caused
417 by prophage-mediated insertional inactivation mutations. Flagella-associated mutations were

418 observed in every (12/12) iron-rich population (irrespective of phage) and were mediated by
419 phage insertional inactivation in every case where phage was present. Under iron-limited
420 conditions, flagella impairment was less common (4/12 populations; 10 clones) and only
421 observed in the presence of phages, where in 9/10 cases this was mediated by prophage
422 insertional inactivation, suggesting that transposable phage promoted the loss of flagellar
423 motility by increasing mutational supply. Lim et al (2012) found that in a closely related
424 species, *Pseudomonas fluorescens,* flagella expression was reduced under iron-limitation.
425 Hence, it is possible that the selective benefit of losing flagella is reduced in iron-limited
426 compared with iron-rich conditions. However, mutations in flagella associated loci have been
427 previously observed in *P. aeruginosa* evolving in an iron-limited liquid culture environment
428 after 150 generations (Kümmerli et al 2015), and in iron-limited artificial sputum medium
429 (Davies et al 2016). In our study, population densities were lower under iron-starvation so the
430 reduced mutation supply may explain the lack of flagella mutations under iron-limitation,
431 which was alleviated by the increased mutational supply afforded by transposable phage
432 (Figure S4).
433
434 Our results also have applied relevance: *P. aeruginosa* is a common cause of chronic lung
435 infections in CF and bronchiectasis, where diverse communities of temperate phages also
436 reside and are associated with disease progression and antimicrobial resistance (Tariq et al
437 2019). Analysis of the sputum of CF patients shows that even within a single sample,
438 coexistence of overproducers alongside nonproducers is common for a variety of *P.*
439 *aeruginosa* virulence-associated phenotypes, such as, pyoverdine, LasA protease and
440 pyocyanin (Mowat et al 2011; O'Brien et al 2017). Crucially, temperate phages, including
441 LESϕ4 used in this study, are active in the CF lung (James et al 2015, Tariq et al 2019),

suggesting that transposable phage may play a role in the generation of genetic diversity in chronic infections.

Acknowledgments

This work was funded by a fellowship from the Centre for Chronic Diseases and Disorders at the University of York to SOB (2015-2017), a Phillip Leverhulme Prize to MAB, the European Research Council under the Grant Agreement No 681295 (RK) and the Swiss National Science Foundation No. 31003A_182499 (RK). We would like to acknowledge support from staff at the Centre for Genomic Research, University of Liverpool and Alexandre Figueiredo for assistance with pyoverdine assays.

References

Anderson, MJ 2001. A new method for non-parametric multivariate analysis of variance. Austral Ecology 26, 32–46

Ankenbauer R, Sriyosachati S, Cox CD. 1985 Effects of siderophores on the growth of Pseudomonas aeruginosa in human serum and transferrin. Infect Immun 49, 132–40

Bollinger N, Hassett DJ, Iglewski BH, Costerton JW, McDermott TR. 2001 Gene Expression in Pseudomonas aeruginosa: Evidence of Iron Override Effects on Quorum Sensing and Biofilm-Specific Gene Regulation. Journal of Bacteriology 183, 1990–1996. (doi:10.1128/jb.183.6.1990-1996.2001)

Breitbart M, Hewson I, Felts B, Mahaffy JM, Nulton J, Salamon P, Rohwer F. 2003 Metagenomic Analyses of an Uncultured Viral Community from Human Feces. Journal of Bacteriology 185, 6220–6223. (doi:10.1128/jb.185.20.6220-6223.2003)

Butaitė E, Baumgartner M, Wyder S, Kümmerli R. 2017 Siderophore cheating and cheating resistance shape competition for iron in soil and freshwater Pseudomonas communities. Nature Communications 8. (doi:10.1038/s41467-017-00509-4)

Cox CD. 1986. Role of pyocyanin in the acquisition of iron from transferrin. Infect Immun 52,263–70

470 Cox CD, Adams P. 1985 Siderophore activity of pyoverdin for Pseudomonas
471 aeruginosa. Infect Immun 48,130–8.
472 Darch SE, West SA, Winzer K, Diggle SP. 2012 Density-dependent fitness benefits in
473 quorum-sensing bacterial populations. Proceedings of the National Academy of Sciences
474 109, 8259–8263. (doi:10.1073/pnas.1118131109)
475 Davies EV, James CE, Williams D, O'Brien S, Fothergill JL, Haldenby S, Paterson S,
476 Winstanley C, Brockhurst MA. 2016 Temperate phages both mediate and drive adaptive
477 evolution in pathogen biofilms. Proceedings of the National Academy of Sciences 113,
478 8266–8271. (doi:10.1073/pnas.1520056113)
479 Diggle SP, Griffin AS, Campbell GS, West SA. 2007 Cooperation and conflict in
480 quorum-sensing bacterial populations. Nature 450, 411–414. (doi:10.1038/nature06279)
481 Diggle SP et al. 2007 The Pseudomonas aeruginosa 4-Quinolone Signal Molecules
482 HHQ and PQS Play Multifunctional Roles in Quorum Sensing and Iron Entrapment.
483 Chemistry & Biology 14, 87–96. (doi:10.1016/j.chembiol.2006.11.014)
484 Dumas Z, Ross-Gillespie A, Kümmerli R. 2013 Switching between apparently
485 redundant iron-uptake mechanisms benefits bacteria in changeable environments. Proc Biol
486 Sci 280, 20131055
487 Smith EE, Buckley DG, Wu Z et al 2006. Genetic adaptation by Pseudomonas
488 aeruginosa to the airways of cystic fibrosis patients. Proc Natl Acad Sci USA 103,8487–92
489 Fothergill JL, Panagea S, Hart CA et al 2007 Widespread pyocyanin over-production
490 among isolates of a cystic fibrosis epidemic strain. BMC Microbiol 7,45.
491 Ghosh D, Roy K, Williamson KE, Srinivasiah S, Wommack KE, Radosevich M. 2009
492 Acyl-Homoserine Lactones Can Induce Virus Production in Lysogenic Bacteria: an
493 Alternative Paradigm for Prophage Induction. Applied and Environmental Microbiology 75,
494 7142–7152. (doi:10.1128/aem.00950-09)
495 Ghoul M, West SA, Diggle SP, Griffin AS. 2014 An experimental test of whether
496 cheating is context dependent. Journal of Evolutionary Biology 27, 551–556.
497 (doi:10.1111/jeb.12319)
498 Ghysels B, Dieu BTM, Beatson SA et al 2004 FpvB, an alternative type I
499 ferripyoverdine receptor of Pseudomonas aeruginosa. Microbiology 150,1671–80.
500 .Granato ET, Ziegenhain C, Marvig RL, Kümmerli R. 2018 Low spatial structure and
501 selection against secreted virulence factors attenuates pathogenicity in Pseudomonas
502 aeruginosa. The ISME Journal 12, 2907–2918. (doi:10.1038/s41396-018-0231-9)

503 Griffin AS, West SA, Buckling A 2004 Cooperation and competition in pathogenic
504 bacteria. Nature 430,1024–7
505 Harrison E, Brockhurst MA. 2017 Ecological and Evolutionary Benefits of Temperate
506 Phage: What Does or Doesn't Kill You Makes You Stronger. BioEssays 39, 1700112.
507 (doi:10.1002/bies.201700112)
508 Harrison F, Buckling A 2007 High relatedness selects against hypermutability in
509 bacterial metapopulations. Proc Biol Sci 274,1341–7.
510 Harrison F, Buckling A. 2005 Hypermutability Impedes Cooperation in Pathogenic
511 Bacteria. Current Biology 15, 1968–1971. (doi:10.1016/j.cub.2005.09.048)
512 Holden VI, Bachman MA. 2015 Diverging roles of bacterial siderophores during
513 infection. Metallomics 7, 986–995. (doi:10.1039/c4mt00333k)
514 Hulo C, Masson P, Le Mercie P & Toussaint, A 2015 A structured annotation frame
515 for the transposable phages: A new proposed family 'Saltoviridae' within the Caudovirales.
516 Virology 477,155-63
517 James CE, Davies EV, Fothergill JL, Walshaw MJ, Beale CM, Brockhurst MA,
518 Winstanley C. 2014 Lytic activity by temperate phages of Pseudomonas aeruginosa in long-
519 term cystic fibrosis chronic lung infections. The ISME Journal 9, 1391–1398.
520 (doi:10.1038/ismej.2014.223)
521 Jansen G, Crummenerl LL, Gilbert F, Mohr T, Pfefferkorn R, Thänert R, Rosenstiel P,
522 Schulenburg H. 2015 Evolutionary Transition from Pathogenicity to Commensalism: Global
523 Regulator Mutations Mediate Fitness Gains through Virulence Attenuation. Molecular
524 Biology and Evolution 32, 2883–2896. (doi:10.1093/molbev/msv160)
525 Jin Z, Li J, Ni L, Zhang R, Xia A, Jin F. 2018 Conditional privatization of a public
526 siderophore enables Pseudomonas aeruginosa to resist cheater invasion. Nature
527 Communications 9. (doi:10.1038/s41467-018-03791-y)
528 Kim M-S, Park E-J, Roh SW, Bae J-W. 2011 Diversity and Abundance of Single-
529 Stranded DNA Viruses in Human Feces. Applied and Environmental Microbiology 77,
530 8062–8070. (doi:10.1128/aem.06331-11)
531 Kümmerli R, Jiricny N, Clarke LS, West SA, Griffin AS. 2009 Phenotypic plasticity of
532 a cooperative behaviour in bacteria. Journal of Evolutionary Biology 22, 589–598.
533 (doi:10.1111/j.1420-9101.2008.01666.x)
534 Kümmerli R, Santorelli LA, Granato ET, Dumas Z, Dobay A, Griffin AS, West SA.
535 2015 Co-evolutionary dynamics between public good producers and cheats in the

536 bacteriumPseudomonas aeruginosa. Journal of Evolutionary Biology 28, 2264–2274.
537 (doi:10.1111/jeb.12751)
538 LaFayette SL, Houle D, Beaudoin T et al 2015 Cystic fibrosis–adapted Pseudomonas
539 aeruginosa quorum sensing lasR mutants cause hyperinflammatory responses. Sci Adv
540 1:e1500199
541 Lamont IL 2003 Identification and characterization of novel pyoverdine synthesis
542 genes in Pseudomonas aeruginosa. Microbiology 149,833–42
543 Lenski RE, Rose MR, Simpson SC et al 1991 Long-Term Experimental Evolution in
544 Escherichia coli . I . Adaptation and Divergence During 2,000 Generations. Am Nat
545 138,1315–41
546 Li H 2013 Aligning sequence reads, clone sequences and assembly contigs with BWA-
547 MEM. arXiv:1303.3997v2
548 Little JW. 2005 Lysogeny, prophage induction and lysogenic conversion. In: Waldor
549 MK, Friedman A, Adhya S, (eds) Phages. ASM Press: Washington DC, pp 37–54.
550 Lim CK, Hassan KA, Tetu SG, Loper, JE & Paulsen, IT 2012 The Effect of Iron
551 Limitation on the Transcriptome and Proteome of Pseudomonas fluorescens Pf-5. PLoS ONE
552 7:e39139
553 Mavrodi DV, Bonsall RF, Delaney SM, Soule MJ, Phillips G, Thomashow LS. 2001
554 Functional Analysis of Genes for Biosynthesis of Pyocyanin and Phenazine-1-Carboxamide
555 from Pseudomonas aeruginosa PAO1. Journal of Bacteriology 183, 6454–6465.
556 (doi:10.1128/jb.183.21.6454-6465.2001)
557 McKenna A et al. 2010 The Genome Analysis Toolkit: A MapReduce framework for
558 analyzing next-generation DNA sequencing data. Genome Research 20, 1297–1303.
559 (doi:10.1101/gr.107524.110)
560 Mowat E, Paterson S, Fothergill JL et al 2011 Pseudomonas aeruginosa population
561 diversity and turnover in cystic fibrosis chronic infections. Am J Respir Crit Care Med
562 183,1674–9
563 O'Brien S, Rodrigues AMM, Buckling A. 2013 The evolution of bacterial mutation
564 rates under simultaneous selection by interspecific and social parasitism. Proc Biol Sci
565 280,20131913
566 O'Brien S, Williams D, Fothergill JL et al 2017. High virulence sub-populations in
567 Pseudomonas aeruginosa long-term cystic fibrosis airway infections. BMC Microbiol 17:30.

Popat R, Harrison F, da Silva AC, Easton SAS, McNally L, Williams P, Diggle SP. 2017 Environmental modification via a quorum sensing molecule influences the social landscape of siderophore production. Proceedings of the Royal Society B: Biological Sciences 284, 20170200. (doi:10.1098/rspb.2017.0200)

Reyes A, Semenkovich NP, Whiteson K, Rohwer F, Gordon JI. 2012 Going viral: next-generation sequencing applied to phage populations in the human gut. Nature Reviews Microbiology 10, 607–617. (doi:10.1038/nrmicro2853)

R Core Team 2016. R: A language and environment for statistical computing. R Foundation for Statistical Computing, Vienna, Austria. URL https://www.R-project.org/.

Sandoz KM, Mitzimberg SM, Schuster M. 2007 Social cheating in Pseudomonas aeruginosa quorum sensing. Proceedings of the National Academy of Sciences 104, 15876–15881. (doi:10.1073/pnas.0705653104)

Sexton DJ, Schuster M. 2017 Nutrient limitation determines the fitness of cheaters in bacterial siderophore cooperation. Nature Communications 8. (doi:10.1038/s41467-017-00222-2)

Strauch E, Kaspar H, Schaudinn C, Dersch P, Madela K, Gewinner C, Hertwig S, Wecke J, Appel B. 2001 Characterization of Enterocoliticin, a Phage Tail-Like Bacteriocin, and Its Effect on Pathogenic Yersinia enterocolitica Strains. Applied and Environmental Microbiology 67, 5634–5642. (doi:10.1128/aem.67.12.5634-5642.2001)

Tariq MA et al. 2019 Temperate Bacteriophages from Chronic Pseudomonas aeruginosa Lung Infections Show Disease-Specific Changes in Host Range and Modulate Antimicrobial Susceptibility. mSystems 4. (doi:10.1128/msystems.00191-18)

Thorvaldsdottir H, Robinson JT, Mesirov JP. 2012 Integrative Genomics Viewer (IGV): high-performance genomics data visualization and exploration. Briefings in Bioinformatics 14, 178–192. (doi:10.1093/bib/bbs017)

Vasse M, Torres-Barceló C, Hochberg ME. 2015 Phage selection for bacterial cheats leads to population decline. Proceedings of the Royal Society B: Biological Sciences 282, 20152207. (doi:10.1098/rspb.2015.2207)

Vasse M, Noble RJ, Akhmetzhanov AR, Torres-Barceló C, Gurney J, Benateau S, Gougat-Barbera C, Kaltz O, Hochberg ME. 2017 Antibiotic stress selects against cooperation in the pathogenic bacteriumPseudomonas aeruginosa. Proceedings of the National Academy of Sciences 114, 546–551. (doi:10.1073/pnas.1612522114)

600 Visca P, Imperi F, Lamont IL 2007 Pyoverdine siderophores: from biogenesis to
601 biosignificance. Trends Microbiol 15,22–30
602 Willner D et al. 2009 Metagenomic Analysis of Respiratory Tract DNA Viral
603 Communities in Cystic Fibrosis and Non-Cystic Fibrosis Individuals. PLoS ONE 4, e7370.
604 (doi:10.1371/journal.pone.0007370)
605 Youard ZA, Wenner N, Reimmann C 2011 Iron acquisition with the natural
606 siderophore enantiomers pyochelin and enantio-pyochelin in Pseudomonas species.
607 BioMetals 24, 513–22
608
609
610
611
612
613
614

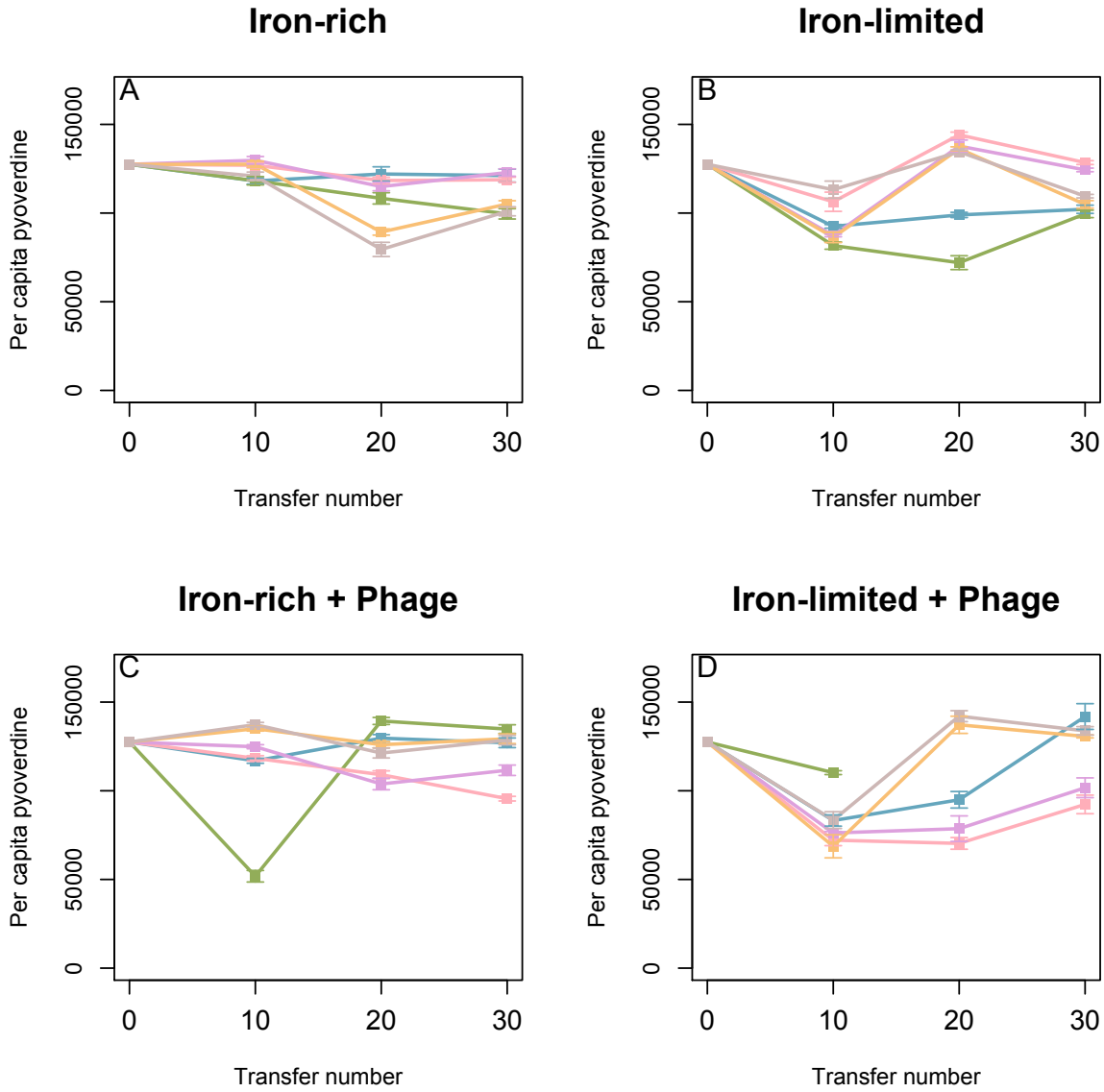

615

616 **Figure 1**

617 Changes in per capita pyoverdine production over the course of 30 transfers for 24
618 populations assigned to one of the following treatments A) iron-rich, B) iron-limited C) iron-
619 rich & phage, D) iron-limited & phage. Iron limitation reduced per capita pyoverdine, but this
620 effect was less strong over time (LMER; iron x transfer interaction, $X^2_{1,9}$= 8.1656, p=0.004).
621 To a lesser extent, phage presence also reduced *per capita* pyoverdine production, but again,
622 this effect was reduced over the course of the experiment (LMER; phage x transfer
623 interaction, $X^2_{1,9}$= 4.2632, p=0.03). The extent to which iron limitation influences pyoverdine
624 production was not influenced by the presence of phage over the course of the experiment,
625 and *vice versa* (LMER; non-significant iron x phage x transfer interaction, $X^2_{1,11}$= 0.0003,
626 p=0.9). Note that one population (green) in the iron-limited and phage treatment (D) went

extinct by timepoint 20. Data show means 30 isolated colonies per population +/- SEM's. Colours represent different evolving populations (1-6) that can be cross-referenced with other figures in this manuscript

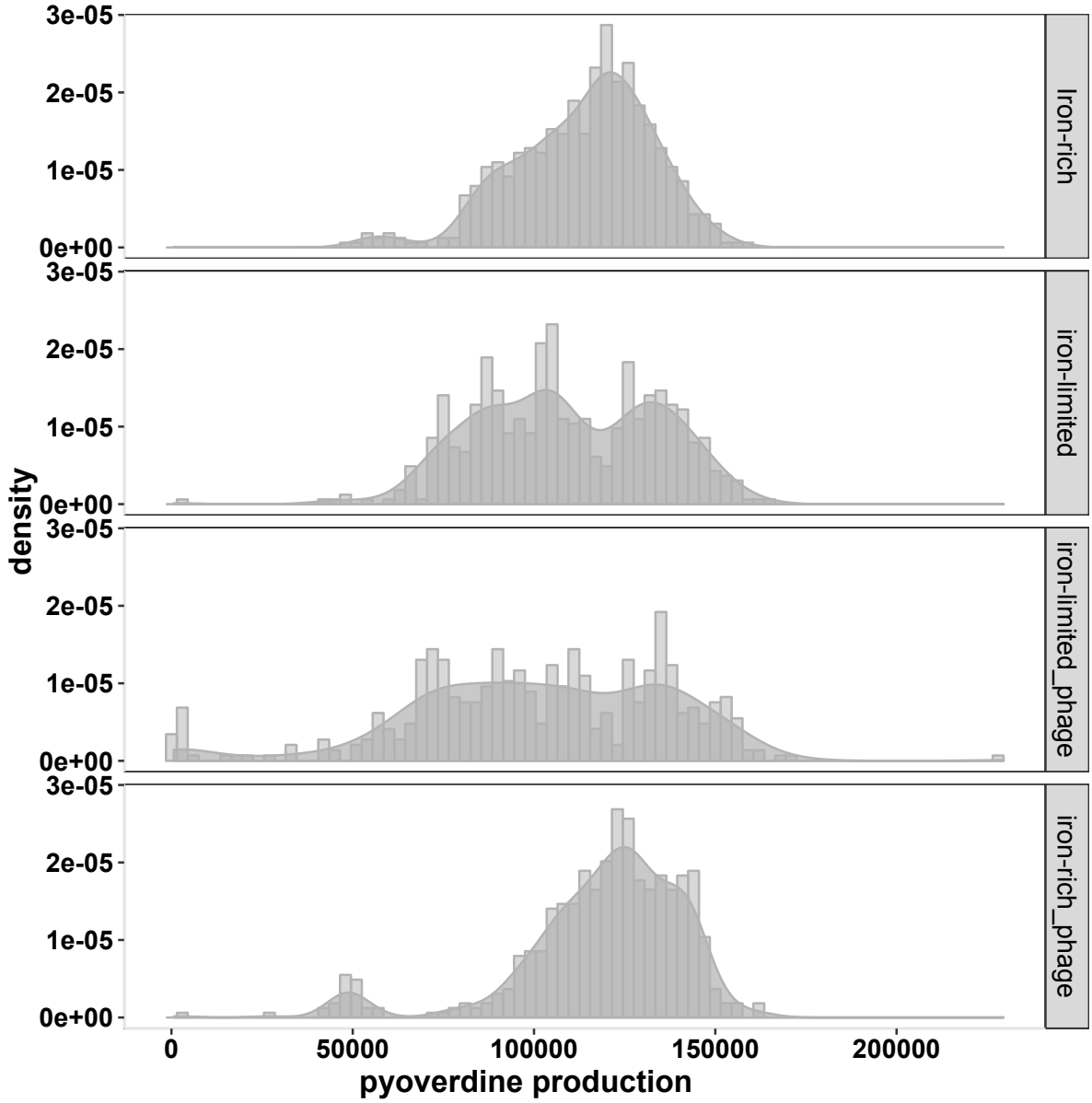

Figure 2

Density histogram illustrating variation in pyoverdine production within each treatment. Data show per capita pyoverdine production for 30 colonies isolated per population at each timepoint (pooling all replicates and timepoints within a treatment). Within-population variance in pyoverdine production increased only under iron-limitation and in the presence of phage (LMER; phage x iron interaction, $X^2_{1,9}$=12.22, p=0.0004), irrespective of time (LMER non-significant phage x iron x transfer interaction $X^2_{1,11}$=0.4591, p=0.4981). Neither iron-limitation nor phage presence alone influenced within-population variance (LMER; iron effect $X^2_{1,6}$= 1.19, p=0.27; phage effect $X^2_{1,6}$= 2.99, p=0.08).

656

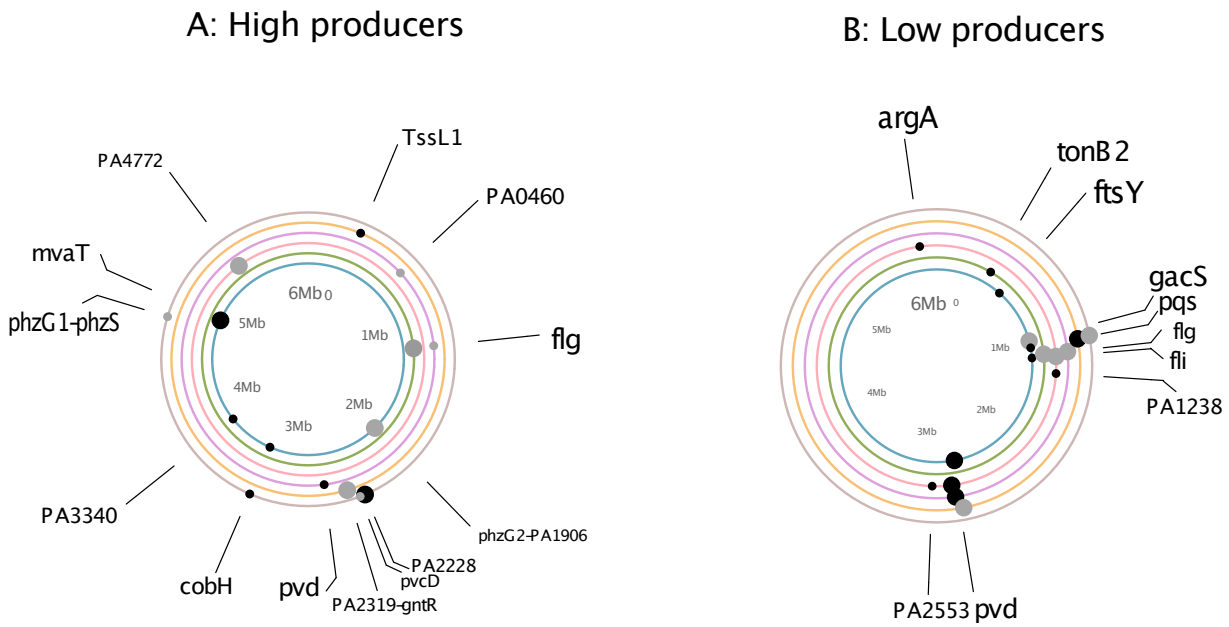

657

658

659 **Figure 3**

660 Genetic loci under positive selection in high (**A**) and low (**B**) pyoverdine producing clones
661 evolving with phages in iron-limited media. Each concentric circle represents a replicate
662 population in either high (**A**) or low (**B**) producers. Concentric circles correspond to
663 populations 1-6, from the innermost to outermost circle, respectively. Colours represent
664 different evolving populations (1-6) that can be cross-referenced with other figures in this
665 manuscript. Positions around each concentric circle correspond to positions around the PAO1
666 published and annotated chromosome. Small black dots around these circles indicate the
667 occurrence of an indel or SNP, grey dots represent phage integration events in those regions,
668 and white dots indicate both. Four colonies were selected in total per population: Dot size
669 corresponds to the number of colonies in which a given mutation was observed. When two
670 genes are mentioned, the mutation is intergenic. A complete list of mutations can be found in
671 Tables S2 and S3.

672

673

674

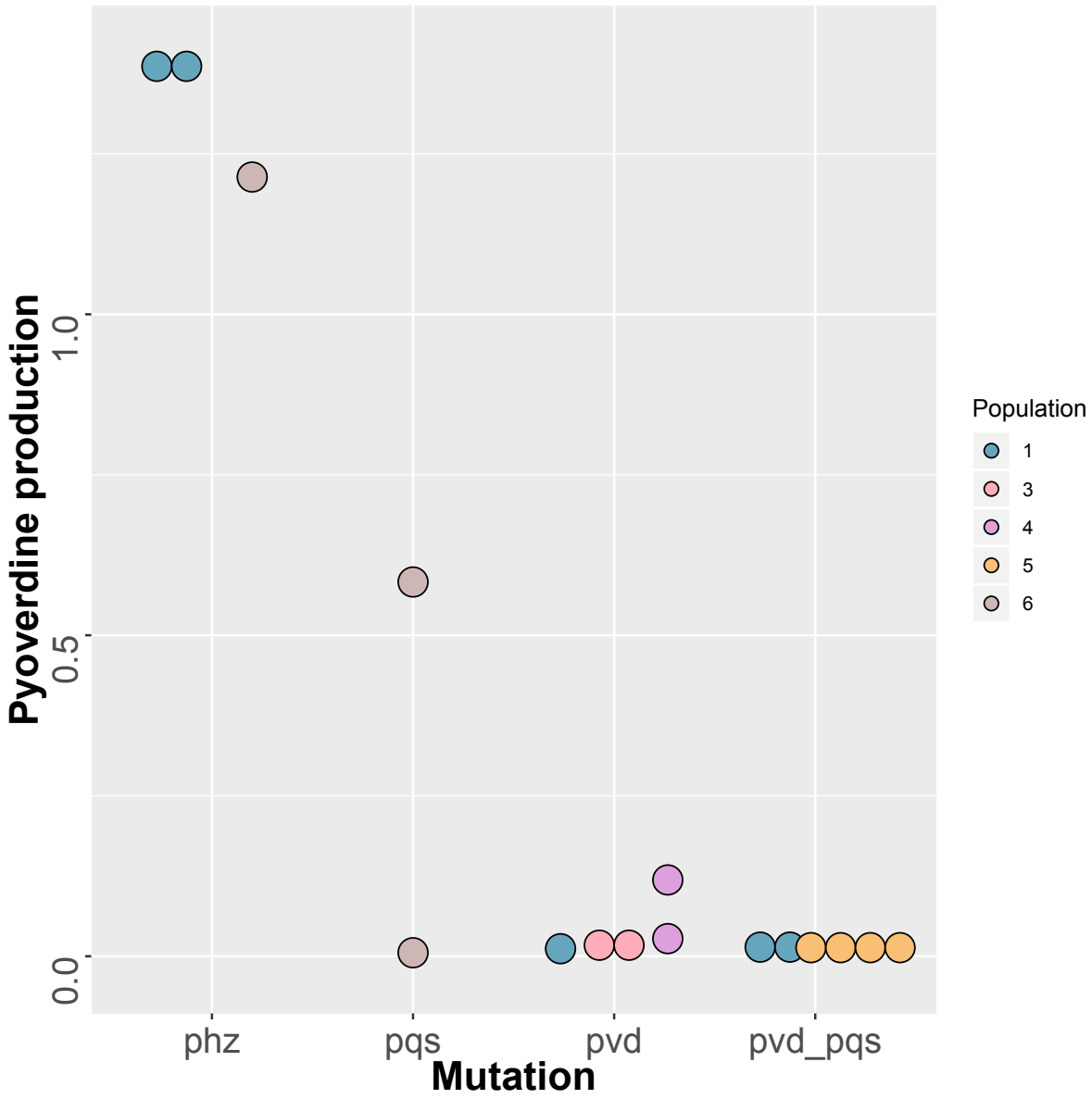

Figure 4

Pyoverdine production relative to ancestor for all clones harbouring mutations in *phz*, *pvd* or *pqs* associated loci in iron-limited population evolving with phage. Clones are colour coded based on the population from which they originate. *Phz* mutants produce higher pyoverdine relative to the ancestor (output > 1), while *pvd* and *pqs* mutations are associated with reduced pyoverdine production (output < 1).